

## Phase stability after an electric-field poling in $\text{Pb}(\text{Mg}_{1/3}\text{Nb}_{2/3})_{1-x}\text{Ti}_x\text{O}_3$ crystals

C.-S. Tu,<sup>1,\*</sup> R. R. Chien,<sup>2</sup> F.-T. Wang,<sup>1</sup> V. H. Schmidt,<sup>2</sup> and P. Han<sup>3</sup>

<sup>1</sup>Department of Physics, Fu Jen University, Taipei, Taiwan 242, Republic of China

<sup>2</sup>Department of Physics, Montana State University, Bozeman, Montana 59717, USA

<sup>3</sup>H.C. Materials Corp., Urbana, Illinois 61802, USA

(Received 20 July 2004; published 23 December 2004)

This work concerns phase thermal stability in (001)-cut  $\text{Pb}(\text{Mg}_{1/3}\text{Nb}_{2/3})_{1-x}\text{Ti}_x\text{O}_3$  crystals after an electric ( $E$ )-field poling, which is crucial for piezoelectric applications. Dielectric properties have been measured as functions of Ti content ( $x=24, 26, 27, 29, 35,$  and  $38\%$ ),  $E$ -field strength, temperature, and poling process. Domain structures after poling have also been observed by polarizing microscopy. An extra dielectric anomaly, which is mostly associated with the appearance of monoclinic domains, was observed during zero-field heating after poling. A prior poling can reveal a “hidden” phase transition which was not clear in unpoled samples. The monoclinic phase plays an essential role in bridging higher symmetries while phase transitions are taking place.

DOI: 10.1103/PhysRevB.70.220103

PACS number(s): 77.84.-s, 77.22.-d, 77.80.Bh

Recent developments on high-strain ferroelectrics  $\text{Pb}(\text{Mg}_{1/3}\text{Nb}_{2/3})_{1-x}\text{Ti}_x\text{O}_3$  (PMNT) have shown that high-quality crystals can be grown and enhance piezoelectricity radically compared with lead zirconate titanate (PZT) ceramics.<sup>1</sup> Physical properties of PMNT are sensitive to Ti content, poling strength, crystallographic orientation, and history.<sup>2-9</sup> The ultrahigh piezoelectric response has been theoretically attributed to polarization rotations between tetragonal ( $T$ ) and rhombohedral ( $R$ ) phases through monoclinic ( $M$ ) or orthorhombic ( $O$ ) symmetries.<sup>10</sup> For piezoelectric performance, an  $E$ -field poling has usually been used before application. However, how poling affects phase stability is still a critical concern for long-term operation.

In pure PMN, an extra peak was observed at  $T_c \sim 212$  K in the field-heating dielectric result, and was attributed to the percolating clusters due to the suppression of the random fields.<sup>11</sup> From synchrotron x-ray diffraction, an  $M_A$ -type  $M$  phase was observed in a (001)-cut PMNT35% crystal after poling ( $E=43$  kV/cm), but the weakly poled sample exhibits an average  $R$  symmetry.<sup>4</sup> From domain observations at room temperature (RT),  $R \rightarrow M_A \rightarrow T_{001}$  and  $R \rightarrow M_A \rightarrow T \rightarrow M_A \rightarrow R_{111}$  transition sequences were evidenced, respectively, in (001)-cut PMNT24% and (111)-cut PMNT33% crystals as  $E$  field increases along oriented directions.<sup>5,6</sup> From the dielectric data, a  $R \rightarrow O \rightarrow T$  transition sequence was suggested for a (011)-cut PMNT33% crystal after poling ( $E < 4$  kV/cm) along [011], but for  $E > 5$  kV/cm a  $R \rightarrow O$  transition was proposed at RT.<sup>7</sup> A field-induced  $R \rightarrow O$  transition via an  $M_B$ -type  $M$  phase was suggested for a (110)-cut PMNT30% crystal.<sup>8</sup>

In this study, the PMNT crystals were grown using a modified Bridgman method. Samples were cut perpendicular to the  $\langle 001 \rangle$  direction. The Ti concentration ( $x\%$ ) was determined by using the dielectric maximum temperature  $T_m$  obtained upon heating (without poling), i.e.,  $x = [T_m(^{\circ}\text{C}) + 10]/5$ .<sup>12</sup> Hereafter,  $x\%$  stands for (001)-oriented PMNT $x\%$ . A Wayne-Kerr Precision Analyzer PMA3260A was used to obtain capacitance. A Janis CCS-450 cold head was used with a Lakeshore 340 controller and the ramping rate was 1.5 K/min. Before any measurement, the sample

was annealed above  $T_m$ . Three processes were used in this study. The first is called “zero-field heating” (ZFH), in which the data were taken upon heating without any  $E$ -field poling. The second process is called “field-cooled zero-field heating” (FC-ZFH), in which the sample was first cooled from the cubic ( $C$ ) phase down to RT with an  $E$  field, then cooled to 100 or 150 K without field before ZFH was performed. In the third process FR-ZFH, the sample was directly poled at RT before ZFH was performed from 100 or 150 K. During the FC or FR, a dc  $E$  field was applied along the orientated direction. The dielectric permittivities shown in the figures were taken at  $f=10$  kHz. The remanent polarization ( $P_r$ ) was measured by using a Sawyer-Tower circuit at  $f=46$  Hz. Domain structures were observed by using a Nikon E600POL polarizing microscope with a crossed polarizer/analyzer (P/A) pair. Transparent conductive films of indium tin oxide (ITO) were deposited on sample surfaces by sputtering. The details for using optical extinction to distinguish various phases for the (001)-cut sample can be found in Ref. 5.

Figure 1(a) shows dielectric results of ZFH and FC-ZFH for 24%. The maximum temperature  $T_m$  was shifted a few degrees higher in the FC-ZFH. Besides a broad maximum near 390 K an extra peak appears near 370 K in the FC-ZFH, whose position (but not the amplitude) is independent of frequency as seen in the inset. The  $P_r$  also exhibits an abrupt decline near 370 K. The coercive field  $E_C$  is  $\sim 3.8$  kV/cm at RT.

ZFH domain structures after the FC, are shown in Fig. 2(a). “ $N$ ” indicates the area without ITO films. When observing the (001)-cut sample along [001] between a crossed P/A pair, the optical extinction angle of the  $R$  phase is  $0^\circ$ .<sup>5</sup> As seen in the inset which shows extinction at  $0^\circ$ , the symmetry of unpoled 24% is mostly  $R$  at 298 K. After the FC, besides the  $R$  domains at 298 K a small fraction of the domain matrix exhibits extinction in the range of  $\sim 20^\circ$ – $70^\circ$ , indicating  $M$  domains (perhaps mixed with  $T$  domains whose extinction angle is  $45^\circ$ ). The unpoled  $\langle 002 \rangle$  x-ray diffraction taken at RT shows a broad peak indicating  $R$  phase, and a distorted  $R$  phase after poling at  $E=6$  kV/cm. Near 371 K,  $M$  domains associated with extinction angles at  $\sim 20^\circ$ – $70^\circ$  expand

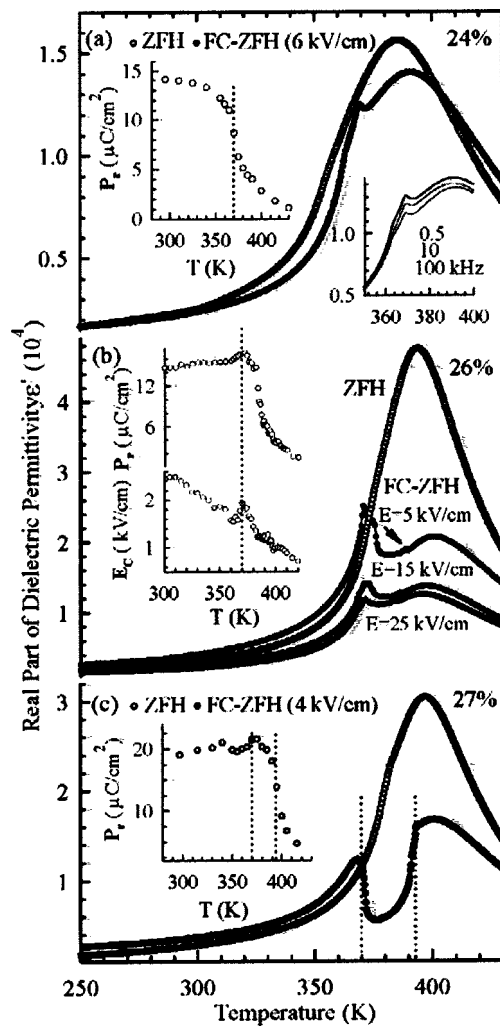
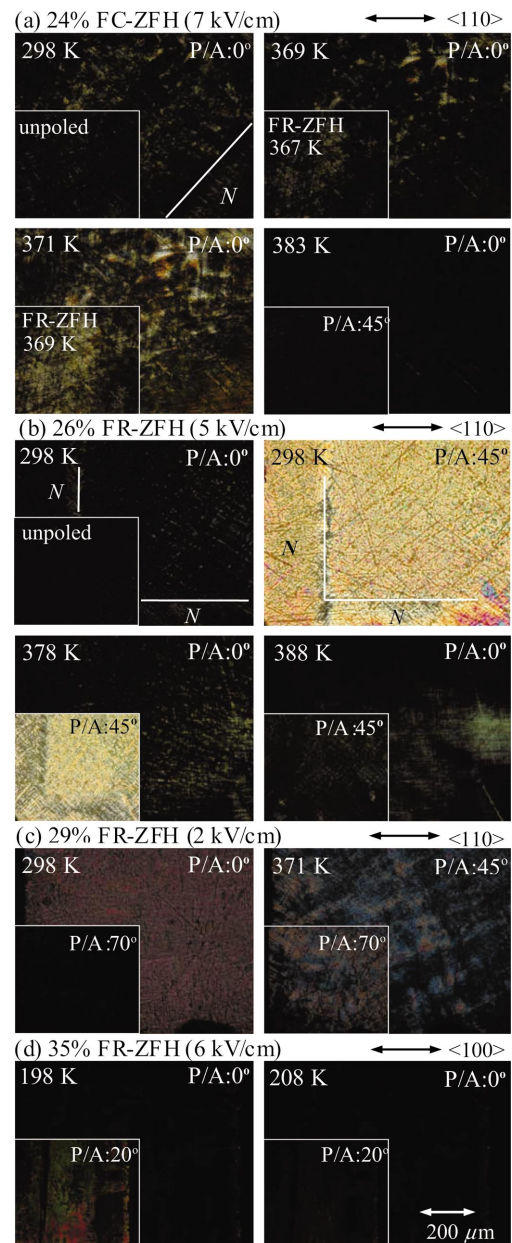


FIG. 1. Dielectric permittivity and remanent polarization.

widely in the domain matrix. This anomaly was also seen in the FR-ZFH [Fig. 2(a)], suggesting that FR and FC have the same poling effect. The crystal turns into cubic near 383 K. Thus, after poling the 24% undergoes a  $R(M) \rightarrow M(R) \rightarrow C$  transition sequence near 370 and 383 K upon heating. “ $R(M)$ ” represents that dominant  $R$  domains coexist with a smaller fraction of  $M$  domains.

More complicated dielectric anomalies were seen in 26%. Compared to the ZFH, in the FR-ZFH two other anomalies as shown in Fig. 1(b), were observed near 370–376 K and  $\sim 385$  K (as indicated by an arrow) which were shifted to lower temperatures with increasing  $E$  field. The minimum  $E$  field to induce this behavior is  $\sim 1.0$  kV/cm, which is smaller than  $E_C \sim 2.5$  kV/cm at RT. As  $E$  field increases, the anomaly seen near 370–376 K becomes a single peak and rather weaker. As shown in Fig. 1(b), the  $P_r$  and  $E_C$  also exhibit a peak near 370 K. Similar dielectric anomalies were observed in the FC-ZFH.

ZFH domain structures after poling are shown in Fig. 2(b). The unpoled sample shows optical extinction at  $0^\circ$  at 298 K, indicating  $R$  domains. In the FR-ZFH, besides the dominant  $R$  domains, a very small fraction of  $M$  domain (with extinction angles of  $\sim 0^\circ - 10^\circ$ ) was observed at


 FIG. 2. (Color) Domain structures. Angles of the P/A pair are with regard to  $[110]$  for 24, 26, and 29 % and  $[001]$  for 35%.

298 K. Near 378 K the  $M$  domains dramatically expand with extinction angles of  $\sim 0^\circ - 15^\circ$ . Near 388 K some domains show extinction at  $45^\circ$ , indicating  $T$  domains. The crystal becomes cubic near 393 K. Similar domain anomalies were seen in the FR-ZFH (10 kV/cm). It is important to note that the “370 K” anomaly was also observed in the pure ZFH domain observation, but not as apparent as in the FR-ZFH. It implies that a prior poling can reveal a “hidden” transition which is not obvious in unpoled samples. The unpoled  $\langle 002 \rangle$  x-ray data [Fig. 3(a)] shows a broad peak and a weak shoulder, which are similar with the  $\langle 002 \rangle$  synchrotron x-ray profile,<sup>3</sup> and likely correspond to  $R$  and  $M$  phases, respectively. The  $M$  phase becomes more pronounced after poling at  $E=5$  kV/cm. Thus, after poling an  $R(M) \rightarrow M(R)$

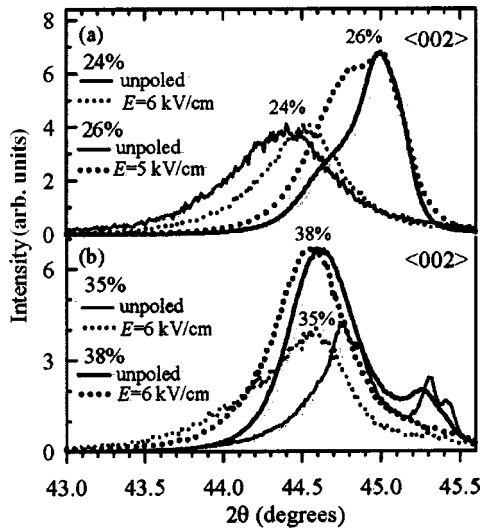


FIG. 3.  $\langle 002 \rangle$  x-ray diffractions taken at RT.

$\rightarrow M(T) \rightarrow C$  transition sequence occurs in 26% near 370–376, 388, and 393 K upon heating.

Similar dielectric anomalies were observed in 27% as given in Fig. 1(c). In the FC-ZFH two clear frequency-independent anomalies (as marked by dashed lines) occurred near 370 and 392 K. The  $P_r$  also shows a maximum peak and a rapid decline near 370 and 392 K. After poling the 27% likely goes through an  $R(M) \rightarrow M(R) \rightarrow M(T) \rightarrow C$  transition sequence near 370, 392, and 400 K upon heating.

Figure 4(a) shows ZFH and FR-ZFH dielectric results for 29%. Besides a broad maximum near 407 K, two extra peaks appear near 358 and 368 K after poling. The minimum  $E$  field to induce this anomaly is  $\sim 2.0$  kV/cm which is smaller than  $E_C \sim 3.3$  kV/cm at RT. The  $P_r$  exhibits an abrupt decline near 365 K. As given in Fig. 2(c), at 298 K domains

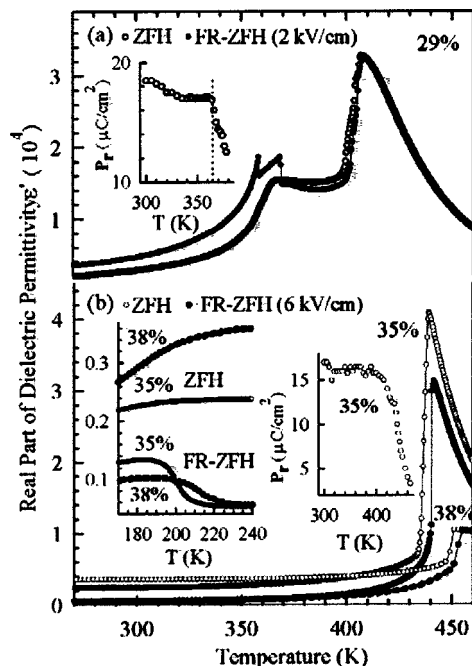


FIG. 4. Dielectric permittivity and remanent polarization.

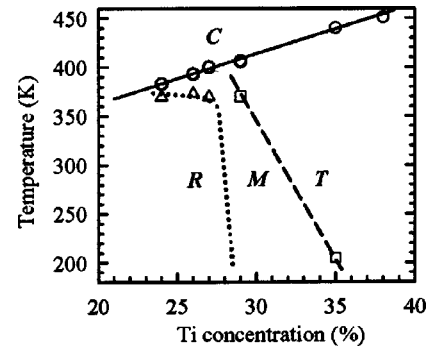


FIG. 5. Phase diagram of (001)-cut PMNT crystals after poling. Triangle and square symbols represent  $R(M) \rightarrow M(R)$  and  $M(T) \rightarrow T(M)$  transitions, respectively. The lines are estimated boundaries for various dominant phases.

show extinction in the range of  $\sim 40^\circ$ – $80^\circ$ , indicating mostly  $M$  domains.<sup>5</sup> At 371 K, besides a small fraction of  $M$  domains associated with extinction at  $\sim 60^\circ$ – $80^\circ$ , most domains exhibit extinction at  $45^\circ$ , indicating  $T$  phase domains.<sup>5</sup> In other words, an  $M(T) \rightarrow T(M)$  transition occurs near 370 K. A similar anomaly was seen in the pure ZFH domain observation. An extra peak occurred near 358 K and weak shoulders appeared in the region of 400–407 K, as seen in Fig. 4(a), that are likely due to phase segregation.

Instead of a gradual rise in the ZFH, the FR-ZFH of 35% in Fig. 4(b) exhibits a steplike decline near 200–210 K. ZFH domain structures observed after poling are shown in Fig. 2(d) for 198 and 208 K. Below 198 K domains exhibit extinction from  $0^\circ$  to  $10^\circ$ , but near 208 K the extinction range becomes twice as wide, i.e.,  $0^\circ$ – $20^\circ$ . A similar anomaly was seen in the pure ZFH domain observation. The  $90^\circ$  domain walls between two domains with their  $T$ -phase polar axes along  $[100]$  and  $[010]$  were seen before the FR process but disappeared after poling.  $T$  and  $M_C$ -type  $M$  domains have extinction at  $0^\circ$  with regard to  $[100]$ .<sup>5</sup> The broad extinction angles ( $0^\circ$ – $20^\circ$ ) imply that polarization directions of  $M$  domains are close to  $[001]$   $T$  polarization. The crystal reaches mostly total extinction at  $E=9$  kV/cm.

The unpoled  $\langle 002 \rangle$  x-ray diffraction [Fig. 3(b)] for 35% exhibits at least four peaks. A dominant  $T$  phase mixed with  $M$  phase was found in the unpoled PMNT35% ceramic.<sup>3</sup> Thus, these peaks likely correspond to  $T$  and  $M$  phase domains. After poling, a strong broad peak and a weak shoulder were observed, perhaps indicating two main  $T$  and  $M$  phase domains. Based on the above evidence, a long-range  $M(T) \rightarrow T(M)$  transition likely takes place in the region of 200–210 K after poling. The crystal becomes cubic near 440 K, where the  $P_r$  exhibits a rapid decline.

A steplike decline was seen near 210 K in the FR-ZFH of 38% [Fig. 4(b)]. This anomaly was not observed for  $E \leq 5$  kV/cm and  $E_C$  is  $\sim 6$  kV/cm at RT. From the ZFH domain observation, a coexistence of  $T$  and  $M$  domains was seen in a 38% in which  $T$  domains increase rapidly from 200 to 300 K.<sup>13</sup> Two peaks were seen in the unpoled  $\langle 002 \rangle$  x-ray diffraction [Fig. 3(b)], perhaps indicating a coexistence of  $T$  and  $M$  domains. After poling, only a broad peak was observed. Note that the  $E$  field was along the  $[001]$   $T$  polar

direction. Thus, the dielectric anomaly seen near 210 K in the FR-ZFH most likely indicates a long-range  $T(M) \rightarrow T$  transition.

This report reveals monoclinic phase stability of (001)-cut PMNT crystals after poling, which depends on Ti content and field strength. The “370 K” dielectric anomaly was seen in 24, 26, and 27 % and correlates to a  $R(M) \rightarrow M(R)$  transition. FC and FR seem to have the same effect on phase transitions as seen upon subsequent ZFH. Figure 5 shows a phase diagram based on this study, where the phase boundaries may be changed with stronger  $E$  field or different crystallographic orientation. It is very different from both the

phase diagram for unpoled PMNT crystals<sup>2</sup> and that obtained from zero-field-cooling and field-cooling results,<sup>9</sup> in which the  $M$  phase was not found. An  $M_C$  phase was found to coexist with  $R$ ,  $T$ , or  $O$  phases in unpoled PMNT ceramics for  $31 \leq x \leq 37$ .<sup>3</sup>  $M_B$  and  $M_C$  phases were also found in unpoled PMNT ceramics for  $27 \leq x \leq 30$  and  $31 \leq x \leq 34$ , respectively.<sup>14</sup>

The authors would like to thank Dr. Haosu Luo for crystals and Professor George F. Tuthill for useful discussions. This work was supported by the DoD EPSCoR Grant No. N00014-02-1-0657 and NSC Grant No. 92-2112-M-030-007.

---

\*Author to whom correspondence should be addressed. Email address: phys1008@mails.fju.edu.tw

<sup>1</sup>S.-E. Park and T. R. Shrout, *J. Appl. Phys.* **82**, 1804 (1997).

<sup>2</sup>T. R. Shrout, Z. P. Chang, N. Kim, and S. Markgraf, *Ferroelectr. Lett. Sect.* **12**, 63 (1990).

<sup>3</sup>B. Noheda, D. E. Cox, G. Shirane, J. Gao, and Z.-G. Ye, *Phys. Rev. B* **66**, 054104 (2002).

<sup>4</sup>Z.-G. Ye, B. Noheda, M. Dong, D. Cox, and G. Shirane, *Phys. Rev. B* **64**, 184114 (2001).

<sup>5</sup>R. R. Chien, V. H. Schmidt, C.-S. Tu, L.-W. Hung, and H. Luo, *Phys. Rev. B* **69**, 172101 (2004).

<sup>6</sup>C.-S. Tu, I.-C. Shih, V. H. Schmidt, and R. Chien, *Appl. Phys. Lett.* **83**, 1833 (2003).

<sup>7</sup>Y. Lu, D.-Y. Jeong, Z.-Y. Cheng, Q. M. Zhang, H. Luo, Z.-W. Yin, and D. Viehland, *Appl. Phys. Lett.* **78**, 3109 (2001).

<sup>8</sup>D. Viehland and J. F. Li, *J. Appl. Phys.* **92**, 7690 (2002).

<sup>9</sup>J. Han and W. Cao, *Phys. Rev. B* **68**, 134102 (2003).

<sup>10</sup>H. Fu and R. E. Cohen, *Nature (London)* **403**, 281 (2000).

<sup>11</sup>V. Westphal, W. Kleemann, and M. D. Glinchuk, *Phys. Rev. Lett.* **68**, 847 (1992).

<sup>12</sup>Z. Feng, H. Luo, Y. Guo, T. He, and H. Xu, *Solid State Commun.* **126**, 347 (2003).

<sup>13</sup>R. Chien, V. H. Schmidt, C.-S. Tu, and L.-W. Hung, *Ferroelectrics* **302**, 581 (2004).

<sup>14</sup>A. K. Singh and D. Pandey, *Phys. Rev. B* **67**, 064102 (2003).